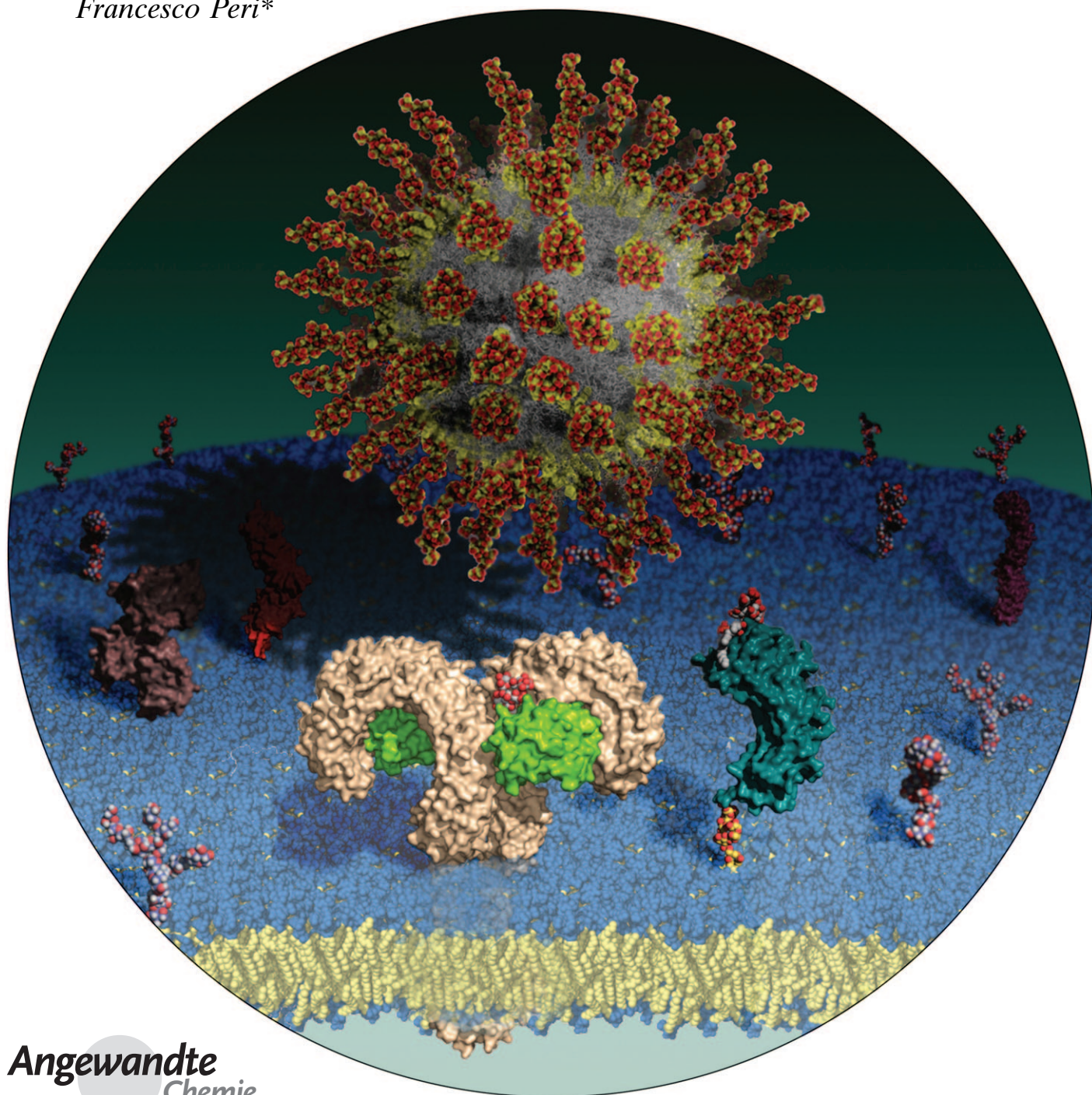


# Uniform Lipopolysaccharide (LPS)-Loaded Magnetic Nanoparticles for the Investigation of LPS–TLR4 Signaling\*\*

Matteo Piazza, Miriam Colombo, Ivan Zanoni, Francesca Granucci, Paolo Tortora, Jerrold Weiss, Theresa Gioannini, Davide Prosperi,\* and Francesco Peri\*

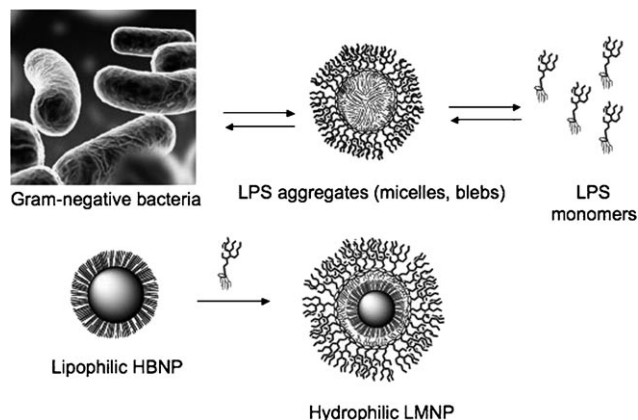


Angewandte  
Chemie

The interaction of highly conserved microbial constituents with the innate immune system contributes greatly to the recognition and reaction against intruding pathogens by mammals. Examples of such microbial constituents include the lipopolysaccharides (LPSs) and lipooligosaccharides (LOSs), also known as endotoxin (E), of Gram-negative bacteria. These potent proinflammatory molecules include a hydrophilic oligosaccharide chain of variable length and a hydrophobic, membrane-anchoring moiety, termed lipid A.<sup>[1–3]</sup> The interaction of E with cells of the innate immune system leads to the formation and release of endogenous mediators, which initiate inflammatory and immune responses essential for optimal antibacterial defense.<sup>[4,5]</sup> Such a cascade of events is triggered by activation of the Toll-like receptor 4 (TLR4) by E. This is the last step of a sequential process of E recognition and interaction with extracellular and cell-surface host proteins, including LPS-binding protein (LBP), soluble and membrane-associated CD14 glycoprotein, secreted and TLR4-associated myeloid differentiation protein 2 (MD-2), and TLR4 itself.<sup>[6–8]</sup>

The amphiphilic character of both LPSs and LOSs results in the formation of micelles in an aqueous environment above their critical micellar concentration (CMC; Scheme 1, top).<sup>[9]</sup> CMC values between  $10^{-8}$  and  $10^{-7}$  M for deep rough mutant LPS Re,<sup>[10,11]</sup> and between 1.3 and 1.6  $\mu\text{M}$  for *Escherichia coli* LPS,<sup>[12]</sup> were reported. In balanced salt solutions containing physiological extracellular concentrations of  $\text{Mg}^{2+}$  and  $\text{Ca}^{2+}$ , CMC values of 1 nM or lower are likely.<sup>[13,14]</sup> From these data and from the fact that LPS aggregates are usually highly stable, aggregated forms of LPS should predominate in the concentration range relevant for biological responses. In physiological fluids, LPS aggregates were also found as membrane “blebs”, which are constitutively released from growing Gram-negative bacteria.<sup>[15]</sup> Transmission electron microscopy (TEM) revealed that blebs exist predominantly as vesicles with an average size of 40–80 nm.<sup>[15]</sup>

The current view of mammalian LPS sensing and signaling is that it is initiated by the LBP-catalyzed extraction and



**Scheme 1.** LPSs or LOSs either extracted and purified or spontaneously released from Gram-negative bacteria form large aggregates (micelles, membrane blebs) in an aqueous environment. LPS-coated magnetic nanoparticles (LMNPs) mimicking LPS aggregates are obtained by coating a hydrophobic brush nanoparticle (HBNP) with bacterial LPS.

transfer of an LPS monomer from aggregates<sup>[16]</sup> to CD14<sup>[17]</sup> and subsequent transfer of the LPS monomer from CD14 to MD-2 or to the MD-2–TLR4 heterodimer.<sup>[7]</sup> While monomeric E–CD14 and E–MD-2 complexes are therefore the proximal vehicles for activation of MD-2–TLR4 and TLR4, respectively, by E, the preceding interactions of host E-binding proteins that preferentially interact with E-rich interfaces and either promote (LBP) or preclude (bactericidal/permeability-increasing (BPI) protein) transfer of E to CD14 play key roles in determining the potency of TLR4 activation by E.<sup>[18]</sup> Accordingly, variables in the aggregation state and the 3D form of E aggregates may directly influence the kinetics and potency of TLR4 activation and signaling.<sup>[9]</sup>

The design of metal-based nanoparticles that possess a suitable rigid size-controlled support for the reversible anchorage of a limited number of E molecules suggests a novel approach to the development of nanoscale vectors for delivery of TLR4 agonists. The potential of integrating inorganic nanoparticles with biomolecular probes has been demonstrated by the creation of targeted contrast agents for magnetic resonance imaging achieved by the conjugation of multiple ligands to iron oxide nanoparticles,<sup>[19]</sup> and by the development of multivalent magnetic relaxation nanosensors for the detection of biomolecules, such as DNA and proteins, and of metabolic activity.<sup>[20–22]</sup> An additional advantage of these particles is the capability of the magnetic core to facilitate the separation of hybrid nanoparticles after ligand conjugation.

Herein, we present the synthesis and application of novel bioactive LPS-coated magnetic nanoparticles (LMNPs). LMNPs were designed to mimic natural E micelles or membrane blebs (Scheme 1, bottom) that contain an E-rich monolayer on the surface with the fatty acyl chains of lipid A oriented inward away from the aqueous surroundings.

The strategies commonly employed for the stable anchorage of organic molecules on the surface of nanoparticles were not appropriate for our purpose, as they usually involve irreversible ligand immobilization or nonspecific physical

[\*] Dr. M. Piazza,<sup>[‡]</sup> M. Colombo,<sup>[‡]</sup> Dr. I. Zanon, Prof. F. Granucci, Prof. P. Tortora, Dr. D. Prosperi, Prof. F. Peri  
Dipartimento di Biotecnologie e Bioscienze, Università di Milano Bicocca  
Piazza della Scienza 2, 20126 Milano (Italy)  
Fax: (+39) 026-448-3565  
E-mail: davide.prosperi@unimib.it  
francesco.peri@unimib.it

Prof. J. Weiss, T. Gioannini  
Department of Internal Medicine, University of Iowa and  
Department of Veterans Affairs Medical Center  
Iowa City, IA 52246 (USA)

[†] These authors contributed equally to this work.

[\*\*] We thank R. Allevi from CMENA for help with TEM images. M.C. acknowledges the research fellowship of CMENA. This work was supported by NIH/NIAID (1R01AI059372), “Regulation of MD-2 function and expression” and “Fondazione Romeo e Enrica Invernizzi”. TLR4 = Toll-like receptor 4. Frontispiece image realized with PyMOL and GIMP by Roberto Cighetti.

Supporting information for this article is available on the WWW under <http://dx.doi.org/10.1002/anie.201004655>.



adsorption onto the nanoparticle surface. The latter typically results in a very unstable hybrid system with unregulated release of the bound molecules and, quite possibly, nonuniform arrangement of the bound ligands on the nanoparticle surface.

To provide nanoparticles that would more likely make possible the stable and reversible binding of a monolayer of E monomers, we designed a hydrophobic brush nanoparticle (HBNP) system with an outer layer of exposed hydrocarbon chains at the surface (Scheme 1). Spherical HBNPs were oleylamine-coated iron oxide nanocrystals, for which a tight control on size and shape could be achieved by wet chemical synthesis.<sup>[23]</sup> HBNPs were resuspended in hexane and added to an aqueous dispersion of commercial LPS (from *E. coli* 055:B5, Sigma, purified by gel-filtration chromatography) at a 5:1 weight ratio. This biphasic mixture was mildly warmed (40 °C) and sonicated to cause the slow evaporation of the organic solvent while mixing. This process promoted the formation of hydrophilic LMNPs with the polysaccharide chains of LPS forming the outer shell. Of the various buffered media tested, dispersion of LPS in 50 mM Tris-HCl buffer with 5 mM ethylenediaminetetraacetic acid (EDTA; pH 7.5) was optimal for the formation of LMNPs.

LMNP stability was dependent on the reaction time and on the initial relative concentrations of HBNPs and LPS in the mixture. These parameters were optimized by monitoring the hydrodynamic size of isolated LMNPs and of the supernatant solutions containing excess LPS. In the absence of HBNPs, LPS micelles had a mean hydrodynamic diameter of 80–100 nm (see Figure S1 in the Supporting Information).

If the coating reaction with LPS was stopped at shorter times, larger size distributions of the recovered particles were observed, possibly reflecting varying aggregation of particles that were only partially covered by LPS. These observed nanoparticle agglomerates of varying size could be reversed (disaggregated) by continued sonication in the presence of LPS until LPS coating was completed. The coating process resulted in stable particle dispersion with a hydrodynamic diameter of  $(193 \pm 4)$  nm. TEM images of LMNPs in water confirmed that the recovered hybrid nanoparticles

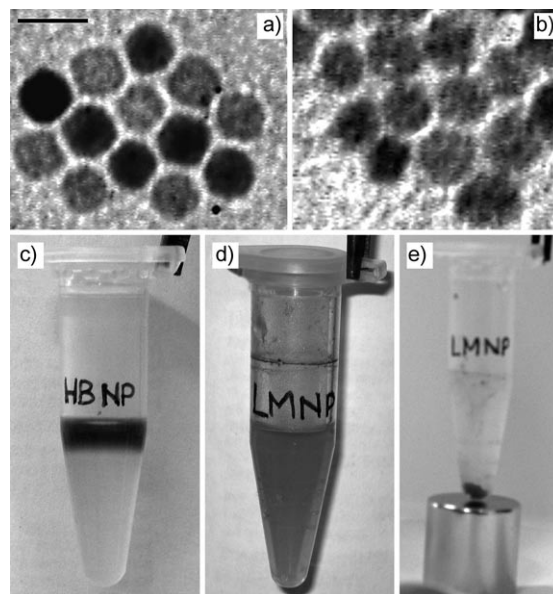


**Figure 1.** TEM images of a) HBNPs in hexane and b) LMNPs in distilled water. Scale bar: 10 nm. c) The upper colored phase is a HBNP dispersion in hexane, while the lower colorless phase is 16.7  $\mu$ M LPS in Tris-EDTA. d) LMNP aqueous dispersion after phase mixing and evaporation of the organic solvent. e) Purification of LMNPs by magnetic decantation.

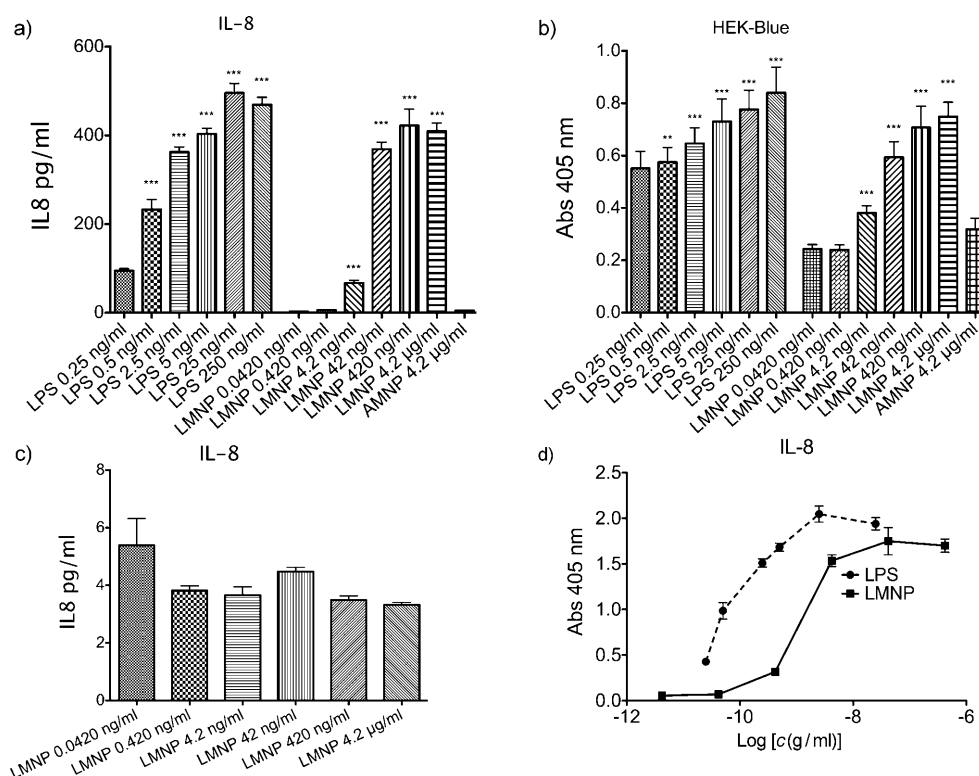


**Figure 2.** a) LMNP-dependent IL-8 production in HEK-TLR4 cells. b) Measurement of LMNP-induced activation of the transcription factor NF- $\kappa$ B level in HEK-Blue cells. c) LMNPs do not stimulate IL-8 production in parental HEK cells. d) Comparison of dose-response curves for LPS and LMNPs from data shown in (a). The results shown represent the mean  $\pm$  standard error of the mean (SEM) of three independent experiments, each in triplicate. The asterisks indicate a significant statistical difference ( $P < 0.01$ ; ANOVA, Dunnett's test) between data in the analyzed group and reference data (LPS 25  $\mu$ M and LMNP 4.2  $\mu$ M for both (a) and (c)).

retained their shape and were generally organized as small clusters of individual particles after solvent evaporation on the sample grid (Figure 1a,b). LMNPs prepared with the described procedure were very stable and could be purified and isolated by magnetic decantation (Figure 1c–e) without apparent loss of water stability once resuspended, even after several purification cycles. Moreover, LMNPs could be stored at 4°C for longer than 1 month and showed no sign of aggregation, as determined by dynamic light scattering, and no degradation in terms of biological activity.

Quantitative evidence of the stability of LMNPs in water and physiological aqueous environments was obtained from relaxivity measurements, as the  $T_2$  value was almost unvaried after 2 hours (see Figure S3 in the Supporting Information). By comparison of the measured  $T_2$  with a standard calibration curve, we could assess the iron content in LMNP dispersions, which was determined to be 1.35 mM Fe. The amount of bound E was quantified by measuring the bound radioactivity of purified LMNPs obtained with the described procedure using tritiated LOS,<sup>[13]</sup> which yielded an estimate that each individual LMNP contained an average of 130 E molecules.

The bioactivity of LPS bound to LMNPs was assessed by measuring the ability of LMNPs to stimulate TLR4-dependent cell activation. Increasing concentrations of LMNPs (from 4.2  $\mu$ M to 4.2 nM of nanoparticle-bound LPS) induced a dose-dependent activation of transformed HEK293 cells expressing CD14, MD-2, and TLR4, as manifested by extracellular accumulation of interleukin-8 (IL-8) from treated “HEK–TLR4” cells (Figure 2a) and of secreted embryonic alkaline phosphatase (SEAP; an NF- $\kappa$ B/AP-1 reporter gene) from treated “HEK–Blue” cells (Figure 2b). In contrast, LMNPs did not activate the parental HEK293 cells that do not express CD14, MD-2, or TLR4 (Figure 2c), thus confirming that activation of HEK–TLR4 and HEK–Blue cells by LMNPs was CD14- and MD-2–TLR4-dependent.

To further define the ability of LMNPs to stimulate TLR4-dependent cellular responses, LMNP-induced activation of cells of the innate immune system was investigated using wild-type (wt), CD14<sup>−/−</sup>, and TLR4<sup>−/−</sup> murine bone-marrow-derived dendritic cells (BMDCs) and bone-marrow-derived macrophages (BMDMs). Cell activation was monitored by the accumulation of extracellular tumor necrosis factor  $\alpha$  (TNF- $\alpha$ ) during incubation for 24 hours. As shown in Figure 3, LMNPs produced dose-dependent activation of both cell types derived from wt mice. The potency of the LMNPs was reduced about tenfold toward CD14<sup>−/−</sup> cells and little or no cell activation was induced by LMNPs in TLR4<sup>−/−</sup> cells. Thus, activation of BMDCs and BMDMs by LMNPs was TLR4-dependent and promoted by CD14, consistent with action of the bound LPS in the LMNPs. This view was further supported by demonstrating that activation of HEK–Blue cells by LMNPs could be inhibited by IAXO-101 (Figure 4), a synthetic glycolipid previously shown to interrupt E-triggered TLR4 activation by antagonizing the LPS–CD14 interaction.<sup>[24,25]</sup>

To verify that the biological activity observed for LMNPs was exclusively related to the immobilized E and not influenced by the inorganic core, we tested LPS-free, water-

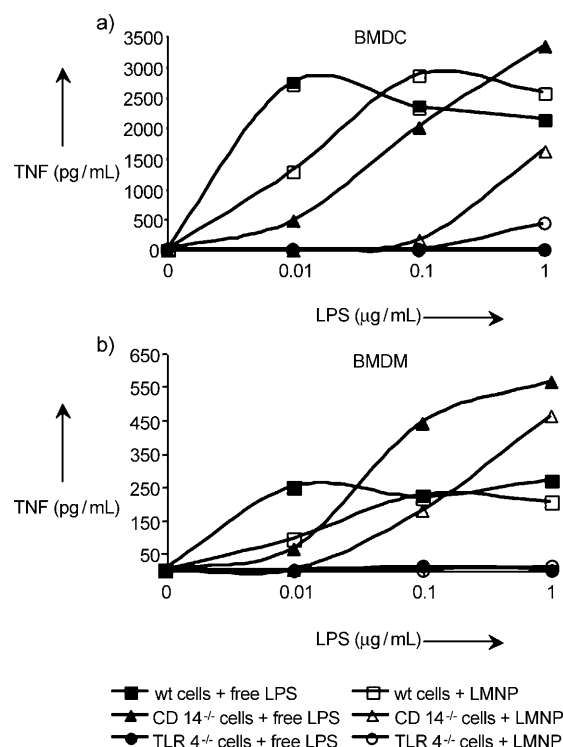


**Figure 3.** LMNP- and free LPS-mediated activation of BMDCs (left) and BMDMs (right). Cells of the innate immune system were activated with LMNPs and the corresponding amounts of free LPS and the release of TNF- $\alpha$  were measured in the supernatant 24 h later. Data are means of at least three independent experiments.

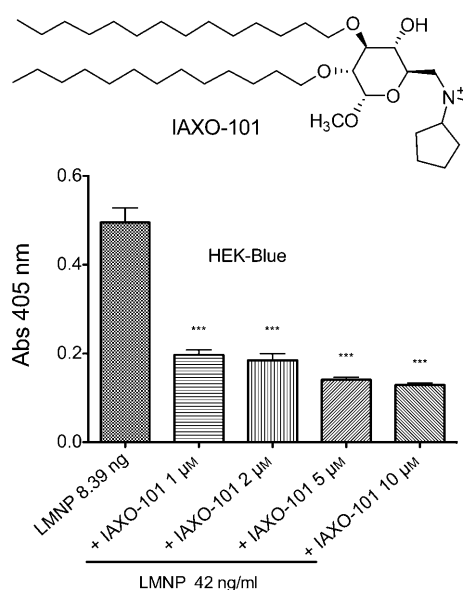


**Figure 4.** Co-administration of LMNPs (42 ng/mL) and increasing amounts of IAXO-101 (0–10  $\mu$ M) to HEK–Blue cells. The results shown represent the mean  $\pm$  SEM of three independent experiments, each in triplicate. The asterisks indicate a significant statistical difference ( $P < 0.01$ ; ANOVA, Dunnett’s test) between data in the analyzed group and reference data (LMNPs alone).

soluble magnetic nanoparticles (MNPs) as a negative control. To this aim, hydrophobic HBNPs were transferred to aqueous

solution by ligand exchange with *N*-phosphonomethyl iminodiacetic acid phosphonate (PMIDA) to give water-soluble anionic MNPs (AMNPs),<sup>[26]</sup> which exhibited a zeta potential of  $-(25 \pm 2)$  mV, very close to that of LMNPs ( $-(18 \pm 3)$  mV). As expected, when treating HEK–Blue cells with AMNPs, no TLR4-dependent SEAP production was observed.

Comparison of the dose-dependent activation by LMNPs and by LPS of HEK–TLR4 and HEK–Blue cells (Figure 2) and of wt and CD14<sup>−/−</sup> murine BMDMs and BMDCs (Figure 3) revealed that the LMNPs were about tenfold less potent than LPS when normalized for the amount of LPS added. Even at the highest dose tested (4.2 nM), LMNPs had no detectable cytotoxic effect (see Figure S4 in the Supporting Information), which indicated that the reduced potency of LMNPs in inducing TLR4-dependent cell activation was most likely due to reduced efficiency of delivery of LPS from LMNPs (versus aggregates of LPS) to CD14 and to MD-2–TLR4 and not a general cytotoxic effect of the LMNPs.

In summary, we have developed an efficient and reproducible synthetic strategy to prepare LMNPs with defined size and shape. The hydrophobic coating of the spherical HBNPs has made possible binding of LPS molecules on the nanoparticle surface in an orientation that resembles the natural presentation of LPS in the outer membrane of Gram-negative bacteria as well as in aggregates of extracted and purified LPS. The LMNPs are stable in solution and the LPS is stably immobilized on the nanoparticles in the absence of suitable E acceptors. LMNPs trigger cell activation in an LPS- and TLR4-dependent manner that is promoted by CD14, which makes it likely that cell activation is dependent on mobilization of LPS monomers from the surface of the LMNPs to MD-2–TLR4. Work is in progress to further investigate the in vitro and in vivo effects of controlled LPS release from LMNPs and the possible application of these reagents as new, nanoparticle-based vaccine adjuvants or immunotherapeutics.

Received: July 28, 2010

Published online: November 9, 2010

**Keywords:** endotoxin · immunology · lipopolysaccharides · nanoparticles · receptors

- [1] M. Freudenberg, T. Merlin, M. Gumenscheimer, C. Kalis, R. Landmann, C. Galanos, *Microbes Infect.* **2001**, 3, 1213.

- [2] H. Heine, E. Rietschel, A. Ulmer, *Mol. Biotechnol.* **2001**, 19, 279.  
 [3] C. Alexander, E. Rietschel, *J. Endotoxin Res.* **2001**, 7, 167.  
 [4] M. Freudenberg, S. Tchapchet, S. Keck, G. Fejer, M. Huber, N. Schütze, B. Beutler, C. Galanos, *Immunobiology* **2008**, 213, 193.  
 [5] B. Beutler, K. Hoebe, X. Du, R. Ulevitch, *J. Leukocyte Biol.* **2003**, 74, 479.  
 [6] T. Gioannini, D. Zhang, A. Teghanemt, J. Weiss, *J. Biol. Chem.* **2002**, 277, 47818.  
 [7] T. Gioannini, A. Teghanemt, D. Zhang, N. Coussens, W. Dockstader, S. Ramaswamy, J. Weiss, *Proc. Natl. Acad. Sci. USA* **2004**, 101, 4186.  
 [8] R. Jerala, *Int. J. Med. Microbiol.* **2007**, 297, 353.  
 [9] T. Gutsmann, A. Schromm, K. Brandenburg, *Int. J. Med. Microbiol.* **2007**, 297, 341.  
 [10] K. Takayama, Z. Din, P. Mukerjee, P. Cooke, T. Kirkland, *J. Biol. Chem.* **1990**, 265, 14023.  
 [11] K. Takayama, D. Mitchell, Z. Din, P. Mukerjee, C. Li, D. Coleman, *J. Biol. Chem.* **1994**, 269, 2241.  
 [12] L. Yu, M. Tan, B. Ho, J. Ding, T. Wohland, *Anal. Chim. Acta* **2006**, 556, 216.  
 [13] P. Giardina, T. Gioannini, B. Buscher, A. Zaleski, D. Zheng, L. Stoll, A. Teghanemt, M. Apicella, J. Weiss, *J. Biol. Chem.* **2001**, 276, 5883.  
 [14] N. Iovine, J. Eastvold, P. Elsbach, J. Weiss, T. Gioannini, *J. Biol. Chem.* **2002**, 277, 7970.  
 [15] D. Post, D. Zhang, J. Eastvold, A. Teghanemt, B. Gibson, J. Weiss, *J. Biol. Chem.* **2005**, 280, 38383.  
 [16] A. Schromm, K. Brandenburg, E. Rietschel, H. Flad, S. Carroll, U. Seydel, *FEBS Lett.* **1996**, 399, 267.  
 [17] R. Schumann, *Res. Immunol.* **1992**, 143, 11.  
 [18] J. Weiss, *Biochem. Soc. Trans.* **2008**, 31, 785.  
 [19] M. G. Harisinghani, J. Barentsz, P. F. Hahn, W. M. Deserno, S. Tabatabaei, C. H. van de Kaa, J. de La Rosette, R. Weissleder, *N. Engl. J. Med.* **2003**, 348, 2491.  
 [20] J. M. Perez, L. Josephson, T. O'Loughlin, D. Hogemann, R. Weissleder, *Nat. Biotechnol.* **2002**, 20, 816.  
 [21] G. Principe, S. Maiorana, P. Verderio, M. Colombo, P. Fermo, E. Caneva, D. Prospero, E. Licandro, *Chem. Commun.* **2009**, 6017.  
 [22] M. Colombo, S. Ronchi, D. Monti, F. Corsi, E. Trabucchi, D. Prospero, *Anal. Biochem.* **2009**, 392, 96.  
 [23] L. Polito, M. Colombo, D. Monti, S. Melato, E. Caneva, D. Prospero, *J. Am. Chem. Soc.* **2008**, 130, 12712.  
 [24] M. Piazza, C. Rossini, S. Della Fiorentina, C. Pozzi, F. Comelli, I. Bettoni, P. Fusi, B. Costa, F. Peri, *J. Med. Chem.* **2009**, 52, 1209.  
 [25] M. Piazza, L. Yu, A. Teghanemt, T. Gioannini, J. Weiss, F. Peri, *Biochemistry* **2009**, 48, 12337.  
 [26] S. Mazzucchelli, M. Colombo, C. De Palma, P. Verderio, M. D. Coghi, E. Clementi, P. Tortora, F. Corsi, D. Prospero, *ACS Nano* **2010**, 4, 5693.